Enhancing di-jet resonance searches via a final-state radiation jet tagging algorithm

Author: Bing-Xuan Liu, Yuxuan Shen, Yuan-Shun-Zi Sui
Speaker: Yuxuan Shen

Sun Yat-Sen University
School of Science

Nov 1, 2025

中山大學 SUN YAT-SEN UNIVERSITY

Our Work

An application of machine learning in di-jet resonance searches

College Students' Innovative Entrepreneurial Training Plan Program

arXiv > hep-ph > arXiv:2510.15151

Search...

Help | Adva

High Energy Physics - Phenomenology

[Submitted on 16 Oct 2025]

Enhancing di-jet resonance searches via a final-state radiation jet tagging algorithm

Bing-Xuan Liu, Yu-Xuan Shen, Yuan-Shun-Zi Sui

In this article, we investigate the possibility of enhancing the di-jet resonance searches by tagging the final state radiation (FSR) jet, using an event-level deep neural network. It is found that solely relying on the 4-momenta of the leading three jets allows the algorithm to achieve good discriminating power that can identify the hardest FSR jet in signal, while rejecting other soft jets. Once the invariant mass is corrected with the tagged FSR jet, the mass resolution of the signal is greatly enhanced, and the sensitivity of the search is also improved by 10-20%. By crafting the input variables carefully, the algorithm introduces minimal mass sculpting for the background, and its applicability extends to a broad mass range. This work proves that FSR jet tagging can potentially enhance the di-jet resonance searches, suiting various stages of the physics programmes at the Large Hadron Collider (LHC) and High-Luminosity LHC (HL-LHC).

https://arxiv.org/abs/2510.15151

中山大學 SUN YAT-SEN UNIVERSITY

Content

Motivation

The Di-jet Search

- **Jets:** Quarks and gluons undergo hadronisation to produce jet-like clusters of particles.
- A heavy particle may decay into two quarks or gluons.
- Use the invariant mass of the leading two jets, m_{jj}, to identify the heavy resonance.
- Sensitive to a broad range of beyond the standard model (BSM) theories.

Z' Boson

- May interact with or decay into dark matter.
- The mediator connecting the SM and BSM.
- A commonly explored benchmark, heavy gauge boson.
- $m_{Z'} \sim$ TeV

Motivation

- FSR jets should be included in the invariant mass calculation
- ISR jets shouldn't be included

ISR and FSR

There can be softer jets from initial-state radiation (ISR) and final-state radiation (FSR).

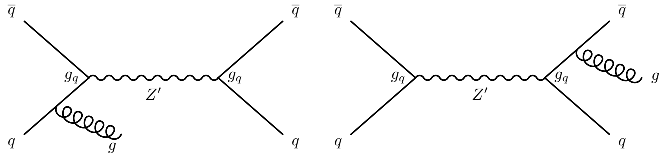

Figure: Feynman diagrams for a heavy Z' particle production in s-channel with an ISR gluon (left) and an FSR gluon (right).

Motivation

FSR Tagging

- Machine learning based
- To distinguish the FSR jets from the ISR jets
- To enhance the sensitivity

Datasets

Tools	Function
MadGraph5_aMC@NLO 2.9.18 Pythia 8.306 Delphes 3.5.3	Samples Generation Showering Event reconstruction

Type	PartonLevel:ISR	PartonLevel:FSR
nominal	on	on
fsr control isr control	off on	on off

Datasets

Signal

Model training: $m_{Z'} = 1 \sim 3\ TeV$, step size $0.5\ TeV$.
Validation: $m_{Z'} = 3.5 \sim 5\ TeV$, step size $0.5\ TeV$.
Each mass point has 250K events.

Background

SM QCD multi-jet events with three slices
cut on leading jet $p_T(4.5, 9, 13.5\ TeV)$.

Comparison of Kinematic Properties -FSR and ISR Jets

The hardest FSR jet should be strongly correlated with the leading two jets.

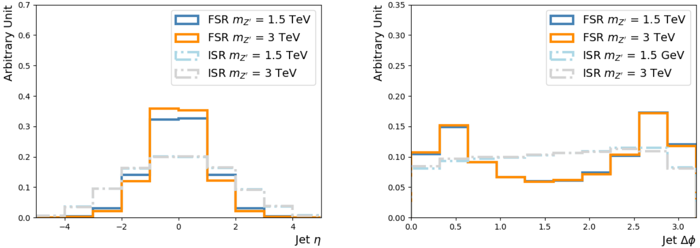

Figure: Selected kinematic distributions of the third jet for the $m_{Z'}$ = 1.5 TeV and 3 TeV samples.

Comparison of Kinematic Properties -FSR and ISR Jets

Mass ratio: $\frac{m^{j3}}{p_T^{j3}}$; p_T ratio: $\frac{p_T^{j3}}{p_T^{j1}}$

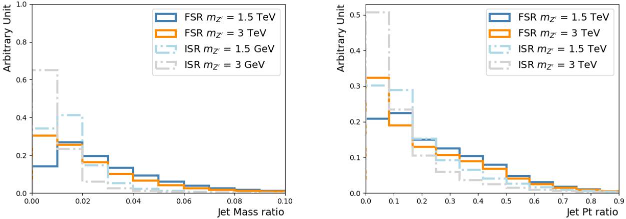

Figure: Selected kinematic distributions of the third jet for the $m_{Z'}$ = 1.5 TeV and 3 TeV samples.

Comparison of Kinematic Properties -Signal and Background

High $m_{\rm jj}$ QCD multi-jet events are dominated by the t-channel production, and the leading two jets are more likely to originate from gluons, compared to the signal.

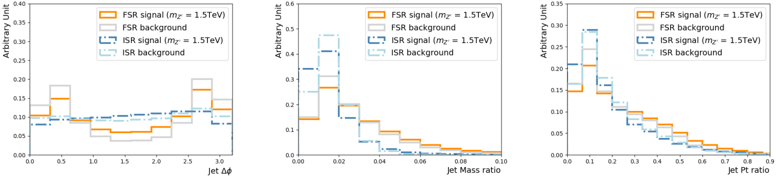

Figure: Selected kinematic distributions of the third jet for the $m_{Z'}$ = 1.5 TeV signal and multi-jet background.

中山大學 SUN YAT-SEN UNIVERSITY

ISR Jet Labelling

We used the nominal samples that have both FSR and ISR jets for the model training. The third jet in the event usually has both ISR and FSR particles associated.

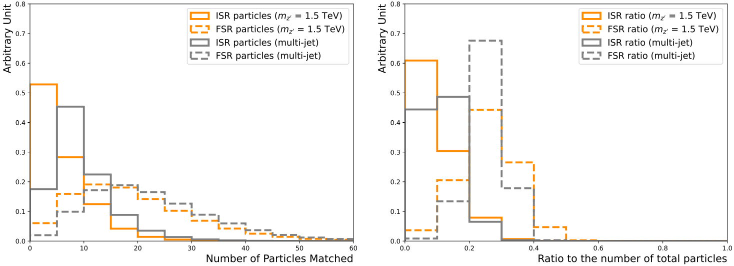

Figure: The number of FSR particles and ISR particles associated with the third jet (left). The ratio of the number of FSR particles and ISR particles to the total number of particles, associated with the third jet (right).

ISR Jet Labelling

The scalar summation of the p_T, Σp_T, can better reflect the origin of the jets. $\frac{\Sigma p_T^{ISR}}{\Sigma p_T^{FSR}} > 1 \Rightarrow ISR\ jet$

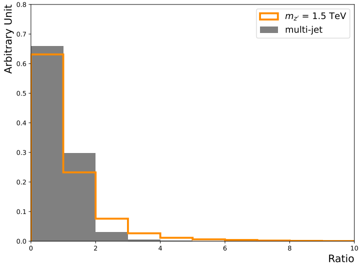

Figure: The ratio between Σp_T of the ISR particles to that of the FSR particles

ISR Jet Labelling

We observed reasonable agreements between the third jet labelled via the above criterion and those in the control samples.

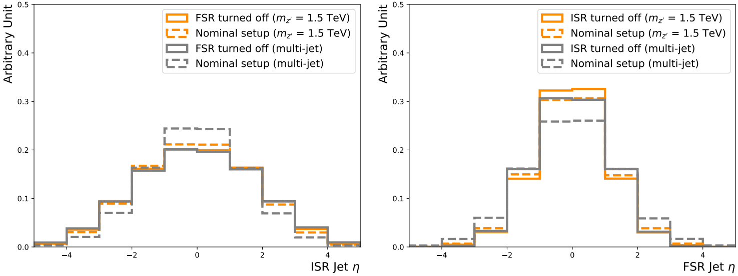

Figure: Comparison of the ISR jet and FSR jet η between those in the nominal sample labelled by the above criterion and those in the corresponding showering control sample.

Network Structure

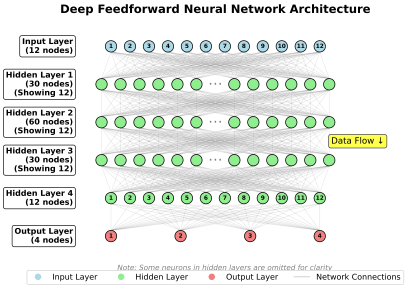

Input Features

Avoid using variables that are strongly correlated with m_{jj}.

$\eta,\ \Delta\phi,\ p_T\ ratio,\ m\ ratio$

Output Variables

Probabilities: $p_s^i, p_s^f, p_b^i, p_b^f$.

Signal: 5 mass points $m_{Z'} = 1 \sim 3\ TeV$ are combined. $\sim$ 460k events.

Background: Multi-jet events with leading jet p_T in $[0.45, 1.75]\ TeV$. $\sim$ 420k events.

batch size: 100 epochs: 100

SGD optimiser with learning rate 0.05

Performance

Build a discriminating variable to balance the target efficiency and the false positive rates:

$$D_{\mathrm{s}}^{\mathrm{f}} = \log \frac{p_{\mathrm{s}}^{\mathrm{f}}}{(f_{\mathrm{s}}^{\mathrm{i}} \cdot p_{\mathrm{s}}^{\mathrm{i}} + f_{\mathrm{b}}^{\mathrm{f}} \cdot p_{\mathrm{b}}^{\mathrm{f}} + (1 - f_{\mathrm{s}}^{\mathrm{i}} - f_{\mathrm{b}}^{\mathrm{f}}) \cdot p_{\mathrm{b}}^{\mathrm{i}})}$$

hyperparameters $f_{\mathrm{s}}^{\mathrm{i}}$ and $f_{\mathrm{b}}^{\mathrm{f}}$ determine the relative importance.

Performance

$$f_{\mathrm{s}}^{\mathrm{i}} = 0.15,\ f_{\mathrm{b}}^{\mathrm{f}} = 0.7$$

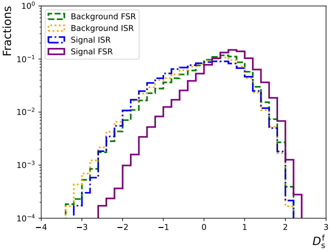

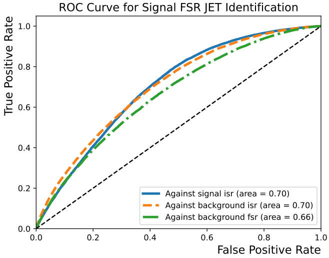

Figure: Left: distributions of the $D_{\mathrm{s}}^{\mathrm{f}}$ for the four categories. Right: "sig-fsr" identification efficiency as functions of the corresponding false positive rates for the three other categories. They are evaluated using the test dataset that accounts for 20% of the total combined dataset.

中山大學 SUN YAT-SEN UNIVERSITY

Application

In an event, if the third jet is identified as coming from the “sig-fsr” category, the m_{jj} is replaced with the tri-jet invariant mass.

- Improved Sensitivity
- Better Mass Resolutions
- Good Generality

Improved Sensitivity

Considering the binned m_{jj}, use the highest value of the significance as an indicator of the sensitivity: $\max\left(\frac{N_s^i}{\sqrt{N_b^i}}\right)$

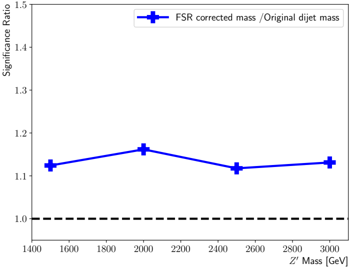

Figure: Summary of the ratios between $\max(\frac{\mathrm{N_s^i}}{\sqrt{\mathrm{N_B^i}}})$ obtained using the FSR corrected mass and that using the original di-jet mass.

Better Mass Resolutions

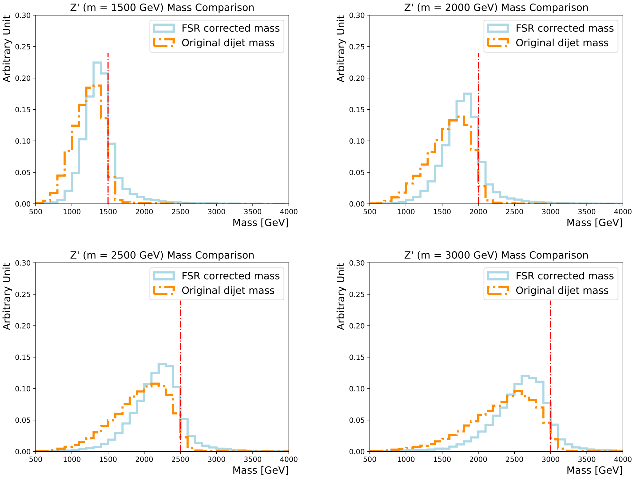

Figure: Comparisons of the FSR corrected masses (solid line) and the original di-jet masses (dotted-dashed line)

Better Mass Resolutions

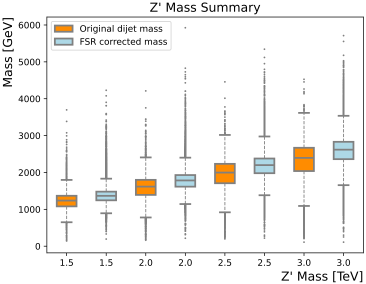

Figure: Summary of the FSR corrected mass distributions (light blue) and the original di-jet masses (dark orange).

Good Generality

The generality of the classifier is assessed using signal points, with $m_{Z'}$ ranging from 3.5 to 5 TeV, that are not included in the training.

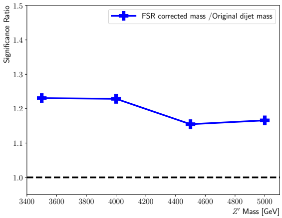

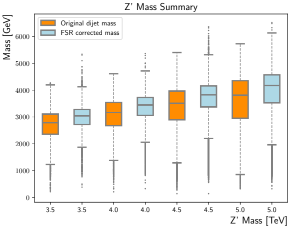

Figure: Left: Summary of the ratios between $\max(\frac{N_s^i}{\sqrt{N_B^i}})$ obtained using the FSR corrected mass and that using the original di-jet mass. Right: Summary of the FSR corrected mass distributions (light blue) and the original di-jet masses (dark orange), for extrapolated signal points.

SUN YAT-SEN UNIVERSITY

Re-defining the Descriminant

$$D_s^f = \log \frac{p_s^f}{(f_s^i \cdot p_s^i + f_b^f \cdot p_b^f + (1 - f_s^i - f_b^f) \cdot p_b^i)}$$

Set $f_s^i = 1$ and $f_b^f = 0$, fully concentrated on distinguishing "sig-fsr" from "sig-isr"

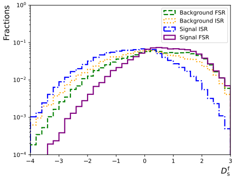

Figure: Distributions of the D_s^f for the four categories

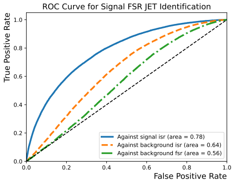

Figure: "sig-fsr" identification efficiency with $f_s^i(f_b^f) = 1(0)$

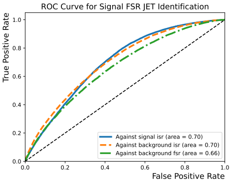

Figure: "sig-fsr" identification efficiency with $f_s^i(f_b^f) = 0.15(0.7)$

中山大學 SUN YAT-SEN UNIVERSITY

Conclusion

A classifier is developed to identify FSR jets in Z' events while rejecting the ISR jets in Z' and FSR/ISR jets in multi-jet background.

- Improvement of 12-20% in the sensitivity of m_{jj}, across a wide mass region.
- 40% sig-fsr identification, around 20% fake rate.
- Flexible to be adapted for different goals.
- Implementation in ATLAS analysis ongoing

Back up

- Simply including softer jets in the mass calculation, without checking whether they are from FSR or ISR, is not a viable strategy.
- It’s sufficient to focus on the hardest fsr jet.

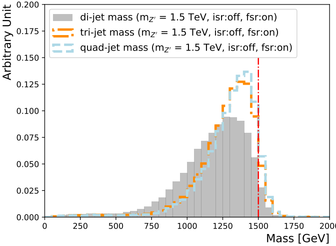

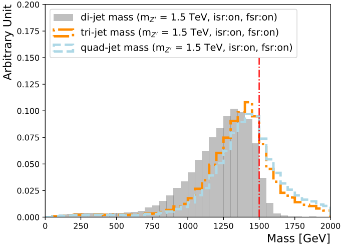

Figure: Comparison of Z’ mass reconstruction with and without third/fourth jet

Input Features

Table: Summary of the input features to train the classifier

Type	Features
angular	$\eta^{j_1}, \eta^{j_2}, \eta^{j_3}, \phi^{j_1}, \phi^{j_2}, \phi^{j_3}$
ratio	$m^{j_1}/p_T^{j_1}, m^{j_2}/p_T^{j_2}, m^{j_3}/p_T^{j_3}, p_T^{j_3}/p_T^{j_1}, p_T^{j_3}/p_T^{j_2}, p_T^{j_2}/p_T^{j_1}$

中山大學 SUN YAT-SEN UNIVERSITY

No Mass Sculpting

The background estimation methods applied in di-jet resonance searches require the background mass to be smoothly falling.

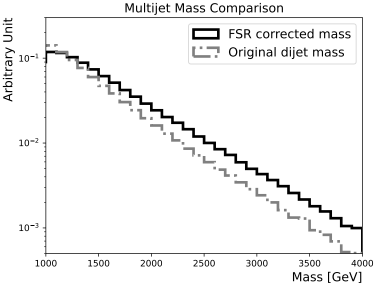

Figure: Comparison of the FSR corrected masses (solid line) and the original di-jet masses (dotted-dashed line), for the multi-jet background.